Materials Letters 139 (2015) 409–413

Contents lists available at ScienceDirect

Materials Letters

journal homepage: www.elsevier.com/locate/matlet

Effect of Si doping on structure, thermal expansion and magnetism of antiperovskite manganese nitrides $Mn_3Cu_{1-x}Si_xN$

Yongjuan Dai [a], Xiaoyan Song [b], Rongjin Huang [c], Laifeng Li [c], Zhonghua Sun [d,*]

[a] School of Materials Science and Engineering, Hebei University of Science and Technology, Shijiazhuang 050000, China
[b] College of Materials Science and Engineering, Key Laboratory of Advanced Functional Materials, Education Ministry of China, Beijing University of Technology, Beijing 100124, China
[c] Key Laboratory of Cryogenics, Technical Institute of Physics and Chemistry, Chinese Academy of Sciences, Beijing 100190, China
[d] Hebei Iron and Steel Technology Research Institute, Hebei Iron and Steel Group, Shijiazhuang 052165, China

ARTICLE INFO

Article history:
Received 19 July 2014
Accepted 25 October 2014
Available online 4 November 2014

Keywords:
Sintering
Magnetic materials
Thermal properties
Ceramics

ABSTRACT

The negative thermal expansion (NTE) performance and correlated structure and magnetism for Si-doped $Mn_3Cu_{1-x}Si_xN$ ($x=0.1$–0.5) are investigated. It is found that the NTE behavior appears below room temperature, the absolute value of coefficient of NTE ($|\alpha|$) tends to be zero and the Curie temperature (T_c) raises rapidly as the increase of Si content. The tendency of T_N temperature depending on Si contents implies that the valence electrons of Si atoms can partially be donated into Mn_{3d}–N_{2p} bond. Another important finding is that positive thermal expansion (PTE), NTE and zero thermal expansion (ZTE) are alternatively appeared by improving the Si content. The present work proposes a novel route to design the low-temperature devices using adjustable NTE or ZTE performance by making use of antiperovskite Mn_3AN materials.

1. Introduction

Materials that contract upon heating, or expand with decreasing temperature within a limited temperature range, are commonly considered to be the negative thermal expansion (NTE) feature. The NTE materials are the indispensable candidates for fabricating the zero thermal expansion (ZTE) devices, which have the potential applications covering the areas from the precision structural parts (e.g. high-precision machinery parts) to the special functional devices (e.g. optical fiber), by means of combining the positive thermal expansion (PTE) compensators [1–5]. Recently, the antiperovskite manganese nitrides (Mn_3AN, A denotes transitional metal elements and/or semiconductor elements) have attracted the attention of physicists and material scientists owing to assembling the isotropic NTE [6–8], the advantageous electric/thermal conductivity [9–11] and the outstanding mechanical performance [12].

To date, it has been known that the NTE behaviors of antiperovskite manganese nitrides are closely correlated with the magneto-volume effect (MVE) [13]. For the original components (e.g. Mn_3CuN [6], Mn_3ZnN [14], Mn_3NiN [15], etc.), they have hardly been considered as the candidates of NTE materials due to either the usual thermal expansion or the sharp volume change. In other words, to obtain the valuable NTE performance, namely, a continuous volume change over a wide temperature range, the gradual development of MVE, which has to be obtained currently by doping the additional atoms on A site [6,13,16,17] or introducing the vacancies into Mn or A site [18,19], is absolutely necessary. In the case of Mn_3CuN, it has been identified that Ge-doped $Mn_3Cu_{1-x}Ge_xN$ or Sn-doped $Mn_3Cu_{1-x}Sn_xN$ are able to exhibit the evidently continuous NTE over a wide temperature range owing to the broadening of MVE [6,16], while the Ga-, Zn-, Ni-, Ag- or In-doped $Mn_3Cu_{1-x}A_xN$ (A=Ga, Zn, Ni, Ag, or In), respectively, are few to express the broadened NTE performance [20]. Significantly, it can be found that the NTE starting temperatures are always moved upward the high-temperature region corresponding to the increase of doping elements. However, few attentions have been paid on the low-temperature NTE behaviors of antiperovskite manganese nitrides [21], where it has extensive applications covering from the microelectromechanical systems in space to the carrying construction of superconducting magnet [17].

We note that Huang et al. found out the continuous NTE behavior below room temperature by partial replacement of Si for Ge in $Mn_3Cu_{0.6}Ge_{0.4-x}Si_xN$ compounds [17]. Regrettably, to date, the further works focusing on the low-temperature NTE properties of antiperovskite manganese nitrides have been rarely investigated. In this letter, we choose the Si-doped $Mn_3Cu_{1-x}Si_xN$ as an example and pay much attention to analyze the effect of Si doping on structure,

* Corresponding author. Tel.: +86 311 86510982; fax: +86 311 86510909.
E-mail address: sunzhonghua@hebgtjt.com (Z. Sun).

http://dx.doi.org/10.1016/j.matlet.2014.10.136
0167-577X/

NTE behavior and magnetism of $Mn_3Cu_{1-x}Si_xN$, and further, propose the mechanism of the low-temperature NTE behaviors and the broadening of MVE as well.

2. Experimental procedures

Polycrystalline samples with the general formula $Mn_3Cu_{1-x}Si_xN$ (x=0.1, 0.2, 0.3, 0.4 and 0.5) were prepared by a solid-state reaction method. The commercial Mn, Cu, Si powders and N_2 gas with the purity of 99.95%, 99.5%, 99.9% and 99.999%, respectively, were used as the starting materials. Firstly, the $Mn_2N_{0.86}$ powder was synthesized according to our previous report [22]. Then, the Cu, Si and $Mn_2N_{0.86}$ powders in accordance with the stoichiometric ratio of $Mn_3Cu_{1-x}Si_xN$ (x=0.1, 0.2, 0.3, 0.4 and 0.5), were homogeneously blended by a high-energy ball milling machine. The ball-to-powder weight ratio of 10:1 was used at a rotation speed of 450 rpm for 12 h. The as-milled powders were pressed into pellets under a pressure of 300 MPa at room temperature, and then sealed in a quartz tube, and sintered at 820 °C under a purified argon atmosphere for 48 h.

The ambient phase constitution was performed by X-ray diffraction (XRD, D/max-3c, Rigaku) with Cu $K\alpha$ radiation. The lattice constant was also achieved by the Rietveld refinement method. The linear thermal expansion data ($\Delta L/L_{(300\ K)}$) was measured using a strain gage over a temperature range of 5–300 K, here, we used fused silica and its corresponding linear thermal expansion data as the reference [23]. The temperature dependence of magnetization was characterized using a superconducting quantum interference device (SQUID) magnetometer and physical property measurement system (PPMS), respectively, under both zero-field-cooled (ZFC) and field-cooled (FC) modes at external magnetic field of 500 Oe.

3. Results and discussion

The room temperature phase constitutions of $Mn_3Cu_{1-x}Si_xN$ (x=0.1, 0.2, 0.3, 0.4 and 0.5) are shown in Fig. 1(a). As seen, all of the $Mn_3Cu_{1-x}Si_xN$ compounds have the predominant phases with antiperovskite Mn_3CuN-type crystal structure (space group $Pm3m$), and the indices of crystallographic plane (hkl) of reflections are also marked. The usual MnO phase is invisible in the present samples. The small signals are determined to be $MnSiN_2$, which is appeared when the Si content is larger than 0.3. The lattice constants of $Mn_3Cu_{1-x}Si_xN$ are calculated by Rietveld refinement [24]. A typical Rietveld refinement of XRD patterns for $Mn_3Cu_{0.8}Si_{0.2}N$ as an example is displayed in Fig. 1(b). Furthermore, the Si content dependence of lattice constant is revealed in Fig. 1(c). As compared, the lattice constant of pure Mn_3CuN is also shown. It can be observed that the lattice constants of $Mn_3Cu_{1-x}Si_xN$ are continuously decreased from 3.907 for x=0 to 3.898 for x=0.5 with increasing the amount of Si doping, which implies that the Cu atoms at the corner positions of Mn_3CuN crystal structure can be successfully substituted by Si atoms. This is because the atomic radius of Si atoms as 1.46 Å is smaller than that of Cu atoms as 1.57 Å, as the replacement of Si for Cu, the cell volumes of $Mn_3Cu_{1-x}Si_xN$ compounds have to be shrunk, and hence, the

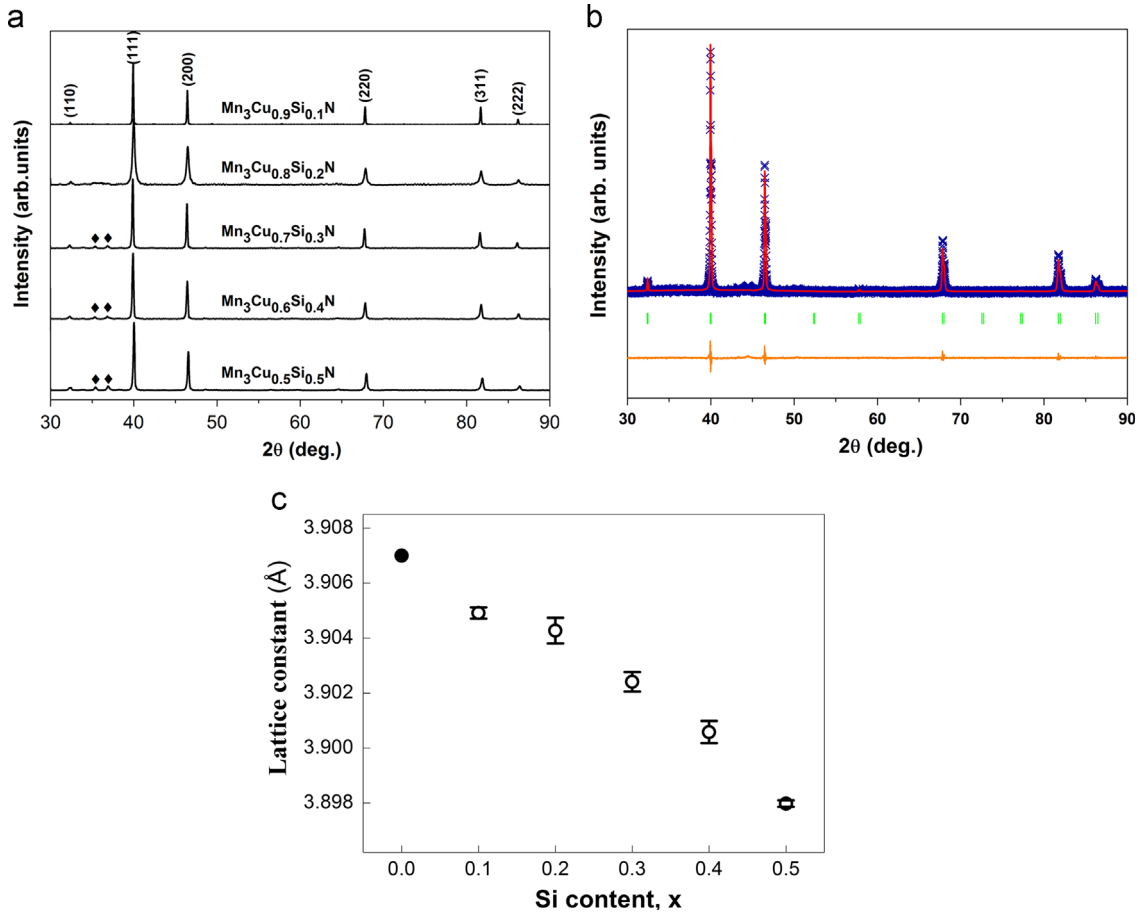

Fig. 1. XRD patterns of $Mn_3Cu_{1-x}Si_xN$ compounds (a), "◆" denotes the $MnSiN_2$ phase; a typical Rietveld refinement of XRD patterns for $Mn_3Cu_{0.8}Si_{0.2}N$ as an example (b), the cross marks and the red solid line show the observed and calculated patterns, respectively, the difference between them is shown at the bottom, the positions of the Bragg reflections are marked by green ticks; Si content dependence of lattice constant (c), "●" indicates the lattice constant of pure Mn_3CuN. (For interpretation of the references to color in this figure legend, the reader is referred to the web version of this article.)

lattice constants of antiperovskite $Mn_3Cu_{1-x}Si_xN$ crystal structure are reduced. The relationship between the Si content and the lattice constant is fit to Vegard's law [25].

It is well-known that the pure Mn_3CuN material does not show NTE due to the absence of MVE [6]. However, the MVE can be occurred by means of Si doping. As shown in Fig. 2a, a small amount of Si doping, e.g. $x=0.1$, can produce a dramatically enhanced MVE, correspondingly, the linear thermal expansion curve of $Mn_3Cu_{0.9}Si_{0.1}N$ increases with decreasing temperature at the temperature range of 122–132 K ($\Delta T=10$ K), i.e. NTE happens, where the coefficient of NTE is $\alpha=-6.3\times10^{-6}\,K^{-1}$ (Fig. 2b). For the further Si doping, the NTE starting temperature alternates from 137 K to 97 K then to 96 K and the slope of NTE declines from $-2.8\times10^{-6}\,K^{-1}$ to $-1.7\times10^{-6}\,K^{-1}$ then to $-0.8\times10^{-6}\,K^{-1}$ in comparable to the Si contents as $x=0.2$, 0.3 and 0.4, respectively (Fig. 2b). The law for the Si content dependence of $|\alpha|$ values indicates that the $|\alpha|$ value is very close to zero as the Si content is equal to 0.4, i.e. zero thermal expansion (ZTE) performance (Fig. 2c). Noticeably, the $Mn_3Cu_{0.7}Si_{0.3}N$ has already reached an ideal ZTE state for $\alpha=-0.001\times10^{-6}\,K^{-1}$ under 30 K (Fig. 2b). However, for a larger amount of Si doping, i.e. $x=0.5$, the NTE behavior is disappeared. The experimental result demonstrates that Si plays an important role in producing the low-temperature NTE performance for Mn_3CuN system.

To understand the low-temperature NTE performance of $Mn_3Cu_{1-x}Si_xN$ as well as the broadening of MVE, the temperature dependence of magnetization is shown in Fig. 3. As seen in Fig. 3 (a), the field-cooled (FC) curve shows a typical ferromagnetism–paramagnetism transition at $T_c=153$ K (T_c is defined as Curie temperature), while no magnetic transition peak appearing in zero-field-cooled (ZFC) curve, which means that the $Mn_3Cu_{0.9}Si_{0.1}N$ has a weak spin-canted ferromagnetism (FM). This result is very consistent with that of Mn_3CuN [26]. Corresponding to the Si contents change from 0.2, 0.3, 0.4 to 0.5, the ZFC curves all exhibit antiferromagnetism (AFM) with the Néel temperatures as $T_N=127$ K, 143 K, 107 K and 77 K, respectively, meanwhile, the FC curves show the Curie temperatures as 160 K, 239 K, 308 K and 367 K (see Fig. 3b–e). Thus, it is known that the T_N temperature is decreased with the increase of Si content. Depending on the empirical knowledge, the T_N temperature in Mn_3AN is determined by the number of valence electrons on A, n_v [10]. As known, Si has four valence electrons ($n_v=4$) while Cu has one ($n_v=1$), when Cu is replaced by Si, the electron concentration of Mn_{3d}–N_{2P} covalent bond should have been enhanced, and then, the T_N temperature has to be increased. As a matter of fact, the present experimental result implies that the Mn_{3d}–N_{2P} covalent bonds probably obtain parts of valence electrons donating by Si atoms. This issue should be understood from two aspects. For one thing, the shrinkage of cell volume (shown in Fig. 1c) probably strengthens the next-nearest-neighbor Mn–N–Mn bonds, which has the potential ability to arrest a number of valence electrons donating by Si atoms; for another, the Si atoms have to donate their valence electrons into the Mn_{3d}–N_{2P} covalent bond. The more is the Si content, the more is the number of valence electrons donated by Si atoms and the more is the number of valence electrons arrested by Mn–N–Mn bonds. As the number of valence electrons arrested by Mn–N–Mn bonds is larger than that of Mn_{3d}–N_{2P} bond absorbing, the T_N temperature is decreased. Consequently, as observed in Fig. 3, the T_N temperature is enhanced when $x=0.2$–0.3, then is reduced when $x>0.3$. Owing to the NTE starting temperature is correlated with T_N temperature, it can be seen in Fig. 2(b) that the NTE behavior is moved toward the low temperature

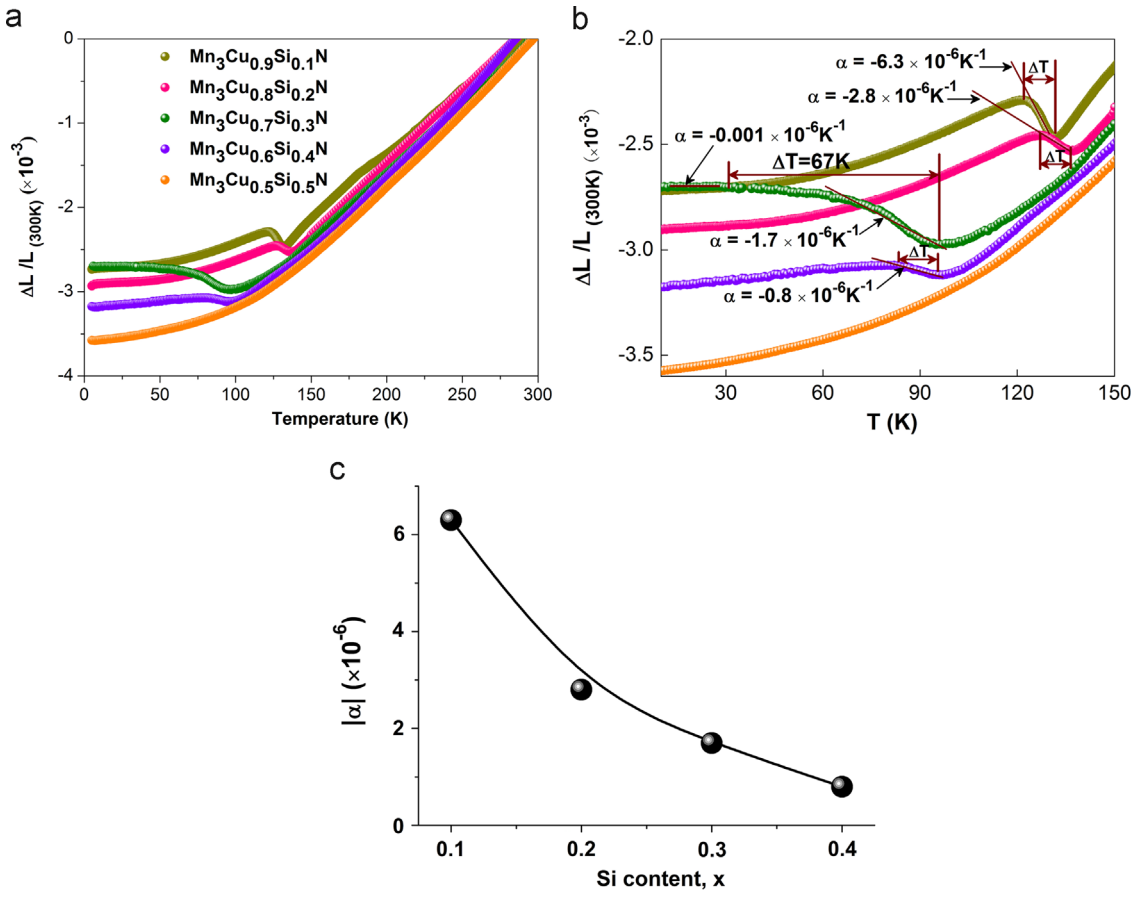

Fig. 2. Negative thermal expansion behavior of $Mn_3Cu_{1-x}Si_xN$. Linear thermal expansion curves of $Mn_3Cu_{1-x}Si_xN$ (a), local amplified NTE behavior (b) and Si content dependence of $|\alpha|$ values (c).

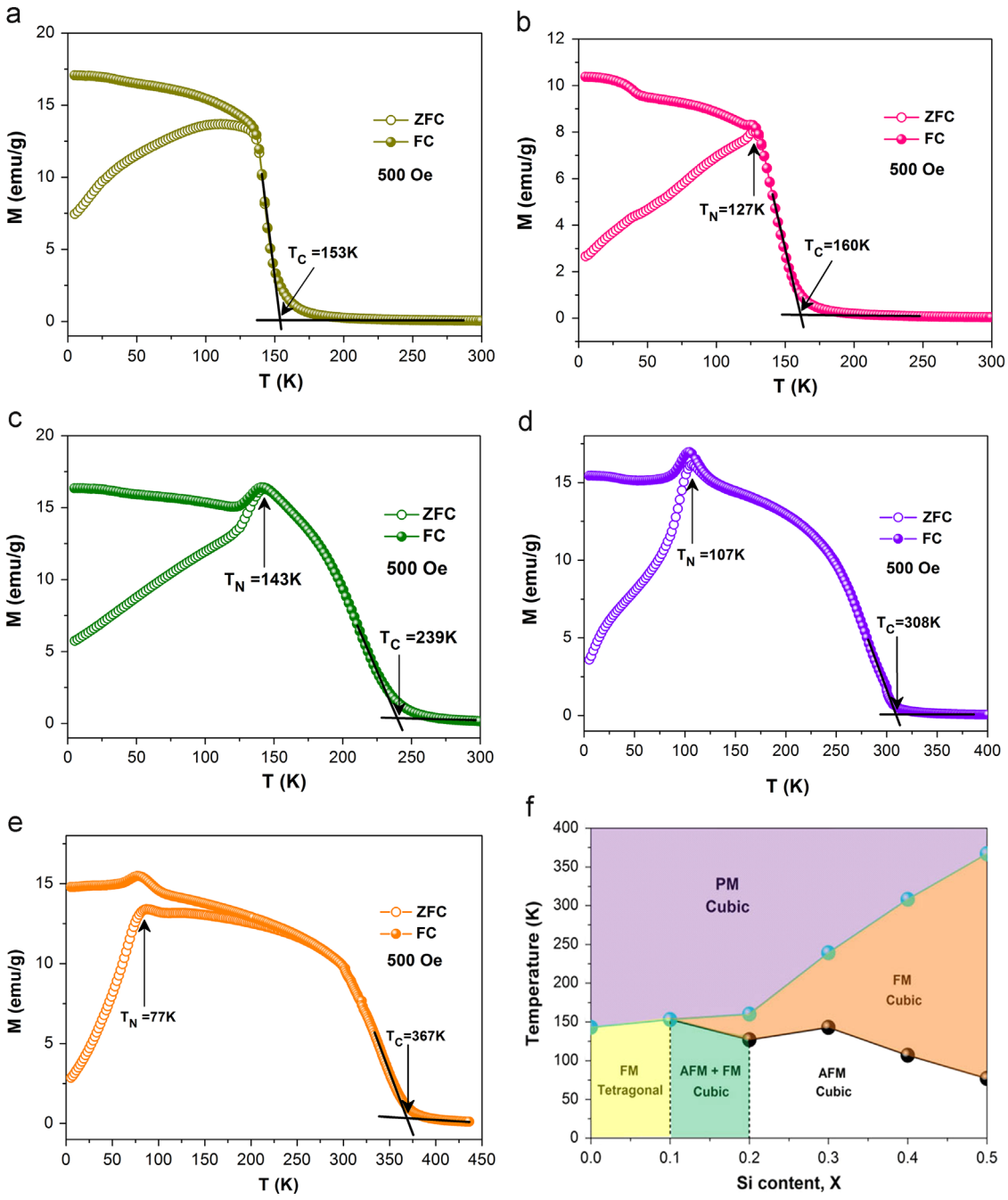

Fig. 3. Temperature dependence of magnetization for $Mn_3Cu_{1-x}Si_xN$, (a) $x=0.1$, (b) $x=0.2$, (c) $x=0.3$, (d) $x=0.4$, (e) $x=0.5$ and (f) structure and magnetic phase diagram of $Mn_3Cu_{1-x}Si_xN$ as a function of Si content.

region with the increase of Si content. As a result of temperature versus magnetization, the structure and magnetic phase diagram of $Mn_3Cu_{1-x}Si_xN$ as a function of Si content is drawn in Fig. 3(f). The structure and magnetism is referenced as those of Mn_3CuN for $x<0.1$ [26,27].

The tendency of NTE operation temperature window depending on Si contents is associated with MVE as well, which results from the exchange interactions between the nearest-neighbor Mn–Mn moments. Due to the fact that the atomic radius of Si is smaller than that of Cu, partial replacement of Cu by Si easily causes the instability of the original inter-atomic attracting and repelling forces between Mn–A atoms [28]. In order to maintain the forces equilibrium between the Mn–Cu atoms and the Mn–Si atoms, the Mn atoms located at the triangular Γ^{5g} structure are inclined to extend the inter-atomic distance. Thus, the antiferromagnetic interactions between the nearest-neighbor Mn–Mn moments have to be weakened, and hence the MVE can be developed slowly against temperature, accordingly, the NTE behavior is gradually extended. The largest ΔT value can achieve 67 K for $Mn_3Cu_{0.7}Si_{0.3}N$ (Fig. 2b). On the other hand, the ferromagnetic interactions between the next-nearest-neighbor Mn–N–Mn moments are enhanced due to the shrinkage of cell volume, thus, the antiferromagnetic interactions between the nearest-neighbor Mn–Mn moments are disturbed. As a result, the MVE is weakened and even disappeared in comparing with the Si content larger than 0.4.

4. Conclusions

The effects of Si doping on the structure, NTE behavior and magnetism of $Mn_3Cu_{1-x}Si_xN$ ($x=0.1$–0.5) are investigated. It is

found that the $Mn_3Cu_{1-x}Si_xN$ compounds exhibit not only the continuously decreasing lattice constants at room temperature but also the abundant thermal expansion behaviors below room temperature, e.g. PTE, NTE and ZTE, by adjusting the Si content. By further optimizing the Si content, the largest ΔT value can be achieved at 67 K for $Mn_3Cu_{0.7}Si_{0.3}N$. Consequently, the present work is proposing a novel route to design the low-temperature devices with adjustable NTE or ZTE performance by making use of antiperovskite Mn_3AN materials.

Acknowledgments

This work was supported by the Open Project of Key Laboratory of Cryogenics, Technical Institute of Physics and Chemistry, Chinese Academy of Sciences (No. CRYO 201309) and the National Natural Science Foundation of China (No. 51101048).

References

[1] Mary TA, Evans JSO, Vogt T, Sleight AW. Science 1996;272:90–2.
[2] Zheng XG, Kubozono H, Yamada H, Kato K, Ishiwata Y, Xu CN. Nat Nanotechnol 2008;3:724–6.
[3] Huang RJ, Liu YY, Fan W, Tan J, Xiao FR, Qian LH, et al. J Am Chem Soc 2013;135:11469–72.
[4] Cairns AB, Catafesta J, Levelut C, Rouquette J, Lee A, Peters L, et al. Nat Mater 2013;12:212–6.
[5] Mostério NCB, Fonseca AF. Phys Rev B 2014;89:195437.
[6] Takenaka K, Takagi H. Appl Phys Lett 2005;87:261902.
[7] Lu NP, Ji AL, Cao ZX. Sci Rep 2013;3:1–6.
[8] Yan J, Sun Y, Wen YC, Chu LH, Wu MM, Huang QZ, et al. Inorg Chem 2014;53:2317–24.
[9] Huang RJ, Chu XX, Wu ZX, Li LF, Xu XD. Appl Phys A 2010;99:465–9.
[10] Huang RJ, Wu ZX, Chu XX, Yang HH, Chen Z, Li LF. Solid State Sci 2010;12:1977–80.
[11] Sun Y, Guo YF, Li J, Wang C, Wang X, Sathish CI, et al. Sci Adv Mater 2014;6:1–5.
[12] Nakamura Y, Takenaka K, Kishimoto A, Takagi H. J Am Ceram Soc 2009;92:2999–3003.
[13] Iikubo S, Kodama K, Takenaka K, Takagi H, Shamoto S. Phys Rev B 2008;77:020409.
[14] Sun Y, Wang C, Huang QZ, Guo YF, Chu LH, Arai M, et al. Inorg Chem 2012;51:7232–6.
[15] Sun Y, Wang C, Chu LH, Wen YC, Nie M, Liu FS. Scr Mater 2010;62:686–9.
[16] Takenaka K, Asano K, Misawa M, Takagi H. Appl Phys Lett 2008;92:011927.
[17] Huang RJ, Li LF, Cai FS, Xu XD, Qian LH. Appl Phys Lett 2008;93:081902.
[18] Song XY, Sun ZH, Huang QZ, Rettenmayr M, Liu XM, Seyring M, et al. Adv Mater 2011;23:4690–4.
[19] Wang C, Chu LH, Yao QR, Sun Y, Wu MM, Ding L, et al. Phys Rev B 2012;85:220103.
[20] Takenaka K, Ichigo M, Hamada T, Ozawa A, Shibayama T, Inagaki T, et al. Sci Technol Adv Mater 2014;15:015009.
[21] Chu XX, Huang RJ, Wu ZX, Chen Z, Li LF. AIP Conference Proceedings; 2012, vol. 1435. p. 393–400.
[22] Sun ZH, Song XY. Mater Lett 2009;63:2059–62.
[23] Kirby RK, Hahn TA, NIST Standard Reference Material 739, Fused-silica Thermal Expansion. Certificate of Analysis (NationalInstitute of Standards and Technology, Washington, 1971).
[24] Dong CJ. Appl Crystallogr 1999;32:838–9.
[25] Lambregts MJ, Frank S. Talanta 2004;62:627–30.
[26] Lin JC, Wang BS, Lin S, Tong P, Lu WJ, Zhang L, et al. J Appl Phys 2012;111:113914.
[27] Takenaka K, Takagi H. Mater Trans 2006;47(3):471–4.
[28] Huang RJ, Li LF, Wu ZX, Chu XX, Xu XD, Qian LH. Solid State Commun 2010;150:1617–20.